Jpn. J. Appl. Phys. Vol. 42 (2003) pp. 5876–5879
Part 1, No. 9A, September 2003

Study of Self-Organized InAs/GaAs Quantum Dots by Photoluminescence and Photoreflectance

Jenn-Shyong HWANG*, Mei-Fei CHEN, Kuang-I LIN, Chiang-Nan TSAI, Wen-Chi HWANG, Wei-Yang CHOU, Hao-Hsiung LIN[1] and Ming-Ching CHEN[1]

Department of Physics, National Cheng Kung University, Tainan, Taiwan
[1]*Electrical Engineering Department, National Taiwan University, Taipei, Taiwan*

(Received October 25, 2002; accepted for publication February 13, 2003)

Using photoluminescence and photoreflectance ranging from 8 to 300 K, this study investigates transition energies in InAs/GaAs quantum dot (QD) samples grown on (100) misoriented 7° towards (110) GaAs substrates using gas source molecular beam epitaxy with various group V/III flux ratios. Only the exciton transition appears in the photoluminescence spectra (PL) of all samples. Experimental results indicate that the decrease in the full width at half maximum (FWHM) of the PL peak with increasing temperature can be attributed to the effective suppression of non-predominant size QD emissions due to carrier tunneling between nearby dots. Signals from all relevant portions of the samples have been observed in the PR spectra. One to three transition energies in QDs, depending on the dot size, are observed in the PR spectra. [DOI: 10.1143/JJAP.42.5876]

KEYWORDS: Quantum Dots, Transition Energy, Photoreflectance, Photoluminescence

In our earlier study, photoluminescence (PL) was used to characterize the self-organized InAs QDs grown on both (100) exact and misoriented 7° toward (110) GaAs substrates by using gas source molecular beam epitaxy (GSMBE).[1] Those results demonstrated that the QD structures grown on misoriented substrates exhibit a better uniformity than those grown on the exact substrates under the same growth conditions. In this study, we apply photoluminescence (PL)[2–5] and photoreflectance (PR) spectra to characterize the self-organized InAs QDs grown on a (100) misoriented 7° toward (110) GaAs substrate by using GSMBE with different group V/III flux ratios (V/III ratio). Only the transition energy of the exciton appears in the PL spectra of all the samples. Conversely, signals are observed in the PR spectra from all the relevant portions of the sample including QDs, the wetting layer (WL), and GaAs sections. In addition to the exciton transition, PR spectra also reveal one to three transitions in the QDs, depending on the dot size.

The QD samples investigated in this study were grown by a VG V80H GSMBE system. High purity hydride AsH_3 and elemental group III sources, In and Ga, were used in the growth. The AsH_3 flow rates were precisely controlled by using a high pressure proportional integral differential system. All samples were grown on (100) misoriented 7° toward (110) semi-insulating GaAs substrates. The sample structures include a 200 nm thick buffer layer grown at 620°C, an InAs layer deposited with a nominal thickness of 3 ML at 490°C, a 10 nm GaAs layer grown at 490°C to avoid In segregation, and a 40 nm GaAs capping layer grown at 620°C. The growth rate was 0.09 ML/s and the V/III ratio during the growth of InAs layer was maintained at 8.2, 4.4, 2.2, and 1.1 for the four samples labeled as C478, C479, C480, and C481, respectively. Table I lists the V/III ratios of these samples. Details of the sample preparation can be found in M. C. Chen *et al.*[1]

PL and PR measurements were performed in a closed cryostate at temperatures ranging from 8 to 300 K to characterize the QD structures. The luminescent signal was dispersed by a monochromator and detected by a Si or Ge photodetector. A standard PR apparatus was used in the PR measurements. The probe beam consisted of a tungsten lamp and a quarter meter monochromator. A He–Cd laser served as the pump beam. The detection scheme consisted of a Si or Ge photodetector and lock-in amplifier. The modulated reflectance signals, $\Delta R/R$ were processed by the lock-in amplifier and a personal computer.

Table I. Sample identification, V/III ratio of InAs layer, thermal quenching energy and activation energy.

sample	V/III ratio	Thermal quenching energy E_Q (meV)	Activation energy E_a (meV)
C478	8.2	10.3	85.0
C479	4.4	9.1	57.7
C480	2.2	10.0	92.6
C481	1.1	9.5	81.8

Figure 1 depicts the PL spectra for all the quantum dot samples at 8 K. According to this figure, the PL peak energy shifts to a lower energy (red shift) as the V/III ratio decreases from 8.2 to 2.2 and then shifts to a higher energy (blue shift) as the V/III ratio is further reduced to 1.1. The red shift of the PL peak energy implies that the QD size increases with a decrease in V/III ratio. This phenomenon is attributed to the decrease in In adatom migration length as the flux rate of AsH_3 increases when the InAs is grown under As-stabilized conditions. The abnormal increase of the PL

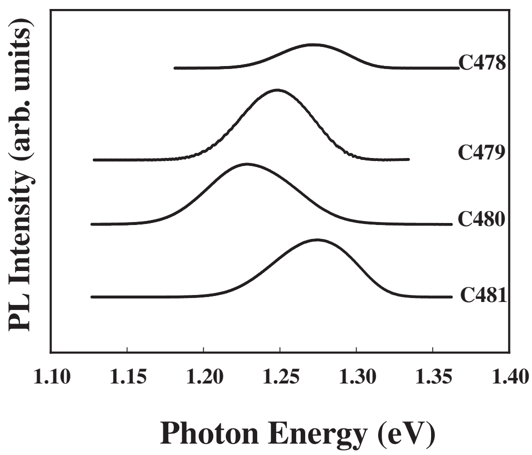

Fig. 1. PL spectra for all samples at 8 K.

*Author to whom all correspondence should be addressed. E-mail: pjshwang@mail.ncku.edu.tw peak energy when the V/III ratio is reduced to 1.1 may be attributed to the change in the growth of InAs from As-stabilized to In-stabilized, thereby enhancing the critical thickness of InAs. In addition, increasing the wetting layer thickness leads to a smaller dot size and higher PL peak energy. Figure 2 shows plots of the wavelength-integrated PL intensity as a function of thermal energy, kT, for all the samples. The integrated intensity as a function of temperature T can be expressed as[1)]

$$I(T) = \frac{I_0}{1 + \exp\left[\dfrac{\Delta E}{E_Q} - \dfrac{\Delta E}{kT}\right]}; \quad (1)$$

where I_0 denotes the integrated intensity at 0 K, ΔE represents the activation energy from the exciton radiative state to the nonradiative state, and E_Q is the thermal quenching energy defined as the thermal energy when the integrated intensity is reduced to half I_0. When the experimental data shown in Fig. 2 are least-squares fitted to eq. 1, ΔE and E_Q can be obtained as fitting parameters. The solid lines in Fig. 2 denote the least-square fits and Table I also includes the obtained values of ΔE and E_Q. Figure 3 shows plots for the full width at half maximum (FWHM) of the PL peaks as a function of thermal energy, kT. With increasing temperature, the FWHM decreases until the thermal energy is comparable to the thermal quenching energy and then, increases as the thermal energy exceeds the thermal quenching energy. In a related study, Lubyshev *et al.* interpreted the behavior of decreasing FWHM in terms of the effective suppression of nonpredominant-size QD emissions due to carrier tunneling between nearby dots.[6,7)] Note that the increase in FWHM at high temperatures are attributed to the increasing effect of the phonon–electron scattering.

Figure 4 displays the PR spectrum of sample C478 at 8 K. The features below the GaAs band gap, 1.52 eV, originate from the QDs and QW in the wetting layer (WL). Meanwhile features observed in the 1.52 to 1.70 eV range are the Franz–Keldysh oscillations (FKOs) originating from the

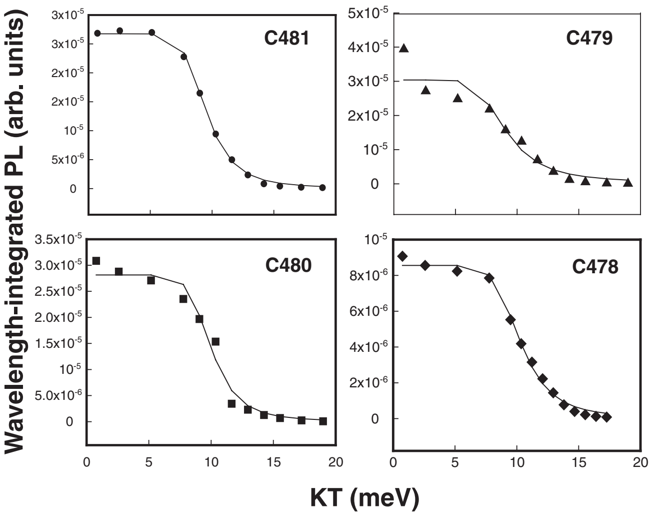

Fig. 2. Wavelength-integrated PL intensity as a function of thermal energy, kT, for all the samples. The solid lines are the least-squares fits to eq. (1).

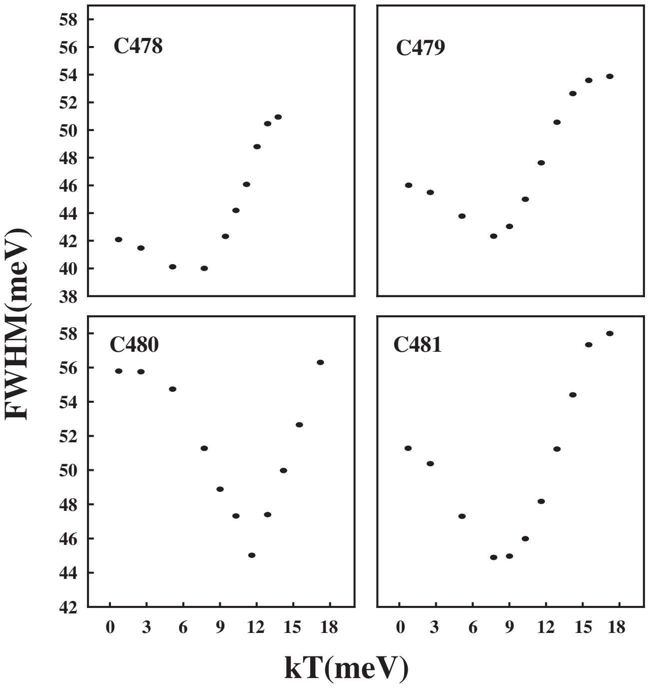

Fig. 3. Full width at half maxima of the PL peaks as a function of thermal energy.

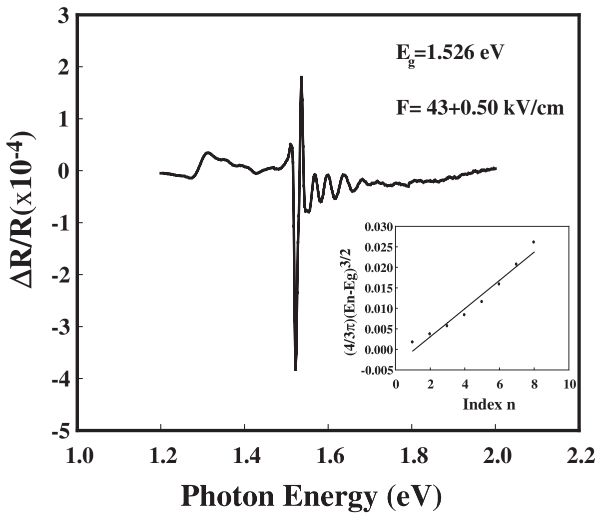

Fig. 4. PR spectrum of the sample C478 at 8 K. The inset is a plot of $(4/3\pi)(E_n - E_g)^{3/2}$ as a function of FKO index n with the least-squares fit shown in solid line.

built-in electric field at the sample's surface. The FKOs disappeared completely when the samples were etched for 2 s by the etching solution that consisted of H_2SO_4, H_2O_2 and H_2O with a volume ratio of 1 : 1 : 50. The etching rate is approximately 36.7 Å/s at room temperature. The inset in Fig. 4 is a plot of $(4/3\pi)(E_n - E_g)^{3/2}$ as a function of FKO index n. Figure 5 displays the features below 1.5 eV of the PR spectra for all the samples at several temperatures. The feature labeled QW corresponds to the electron-heavy hole transition energy of the quantum well formed in the wetting layer while the features designated QD1, QD2, and QD3 originate from the QDs. The lowest energy signal, labeled exciton, is the energy of the confined exciton in the self-

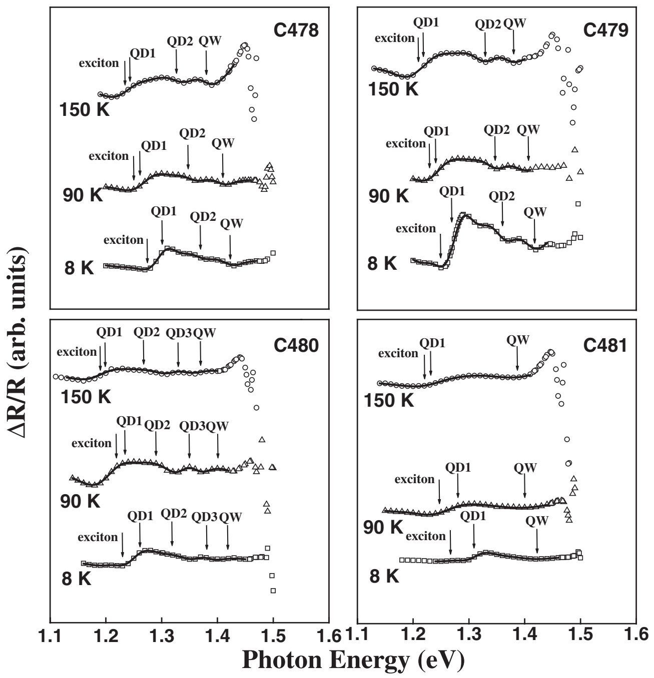

Fig. 5. Features of the PR spectra shown in detail below 1.5 eV for all the samples at several temperatures. The solid lines represent the least-squares fits to their corresponding lineshape with the transition energies indicated by arrows.

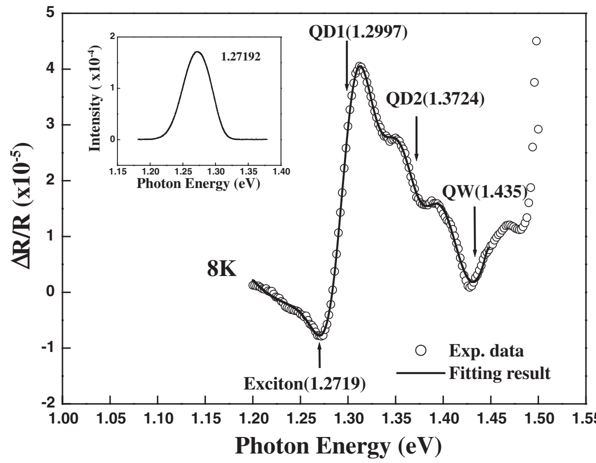

Fig. 6. The detailed fitting to the first derivative Gaussian lineshape for all features originating from QDs and QW in the PR spectrum of sample C478 at 8 K. Shown in the inset is the PL spectrum.

organized InAs quantum dots. The PR spectra were well fitted to the first derivative of a Gaussian profile to accurately determine the transition energies of each feature. Arrows in Fig. 5 denote the obtained transition energies of the features, while solid lines represent the curves of the least-squares fits. To ensure that these solid lines are discernible, one out of every three data points has been removed from the data curves. Table II lists the exciton energies obtained from the PR spectra for all the samples at various temperatures along with the peak energies of the PL spectra. According to the table, results obtained for the PL spectra correlate well with those for the PR spectra. Figure 6 illustrates the detailed fitting to the first-derivative Gaussion lineshape for all the features originating from the QDs and QW in the PR spectrum of sample C478 at 8 K. The inset in Fig. 6 is the PL spectrum. Notably, the exciton energies in the PR and PL spectra are identical.

The $\boldsymbol{k} \cdot \boldsymbol{p}$ method was employed to calculate the theoretical transition energies in the strained layer of InAs/GaAs QW structures with 1.5 ML width.[8] Parameters used in the calculation, including the band gap, deformation potential, elastic constant, and effective mass can be found in refs. 9 and 10. The band offsets are 0.25 and 0.17 eV for the conduction band and valence band, respectively. According to Fig. 7, the experimental and theoretical QW transition energies for all samples at various temperatures closely correspond to each other. This figure also includes the transition energies of QDs and the exciton. Notably, two QD transitions, labeled QD1 and QD2, appeared in the PR

Table II. Comparison of exciton energies obtained from PR and PL measurements.

Temperature (K)	C478 PL (eV)	C478 PR (eV)	C479 PL (eV)	C479 PR (eV)	C480 PL (eV)	C480 PR (eV)	C481 PL (eV)	C481 PR (eV)
8.8	1.272	1.271	1.248	1.248	1.232	1.234	1.273	1.274
30	1.270	1.270	1.248	1.248	1.232	1.229	1.272	1.271
60	1.263	1.263	1.241	1.241	1.228	1.228	1.265	1.265
90	1.251	1.251	1.229	1.229	1.218	1.220	1.251	1.251
105			1.223	1.223	1.211	1.212	1.242	1.242
110	1.244	1.244						
120	1.241	1.240	1.217	1.217	1.204	1.205	1.235	1.231
130	1.238	1.237						
135			1.212	1.212	1.194	1.194	1.228	1.222
140	1.236	1.236						
150	1.235	1.235	1.209	1.208	1.189	1.189	1.223	1.211

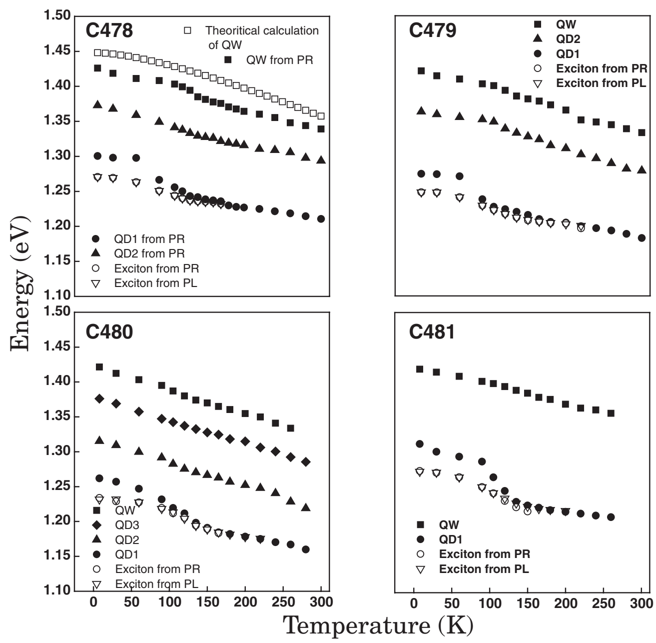

Fig. 7. Transition energies obtained from the PR spectra for all samples at various temperatures. The curve shown in open squares (□) in C478 represents the theoretical transition energies originating from QW for all samples.

spectra of samples C478 and C479. Meanwhile, three transitions, labeled QD1, QD2, and QD3, are observed in the PR spectrum of sample C480 that has QDs larger than those of C478 and C479. As mentioned earlier, sample C481 has the smallest QDs because it was grown with a V/III ratio of 1 : 1 which is under In-stabilized growth conditions. Therefore, only a single QD transition was observed in the PR spectrum of sample C481. The exciton feature gradually disappears when the temperature surpasses 110 K or when the thermal energy (kT) is larger than the thermal quenching energy ($\approx$10 meV).

In conclusion, this study investigated the transition energies in InAs/GaAs QD samples grown on (100) misoriented 7° toward (110) GaAs substrates using GSMBE with various V/III ratios by PL and PR spectra ranging from 8 to 300 K. For all the samples at all different temperatures, PL spectra revealed only one optical transition originating from the confined exciton. Only one predominant QD is formed in the samples and the dot size depends on the V/III ratio or the AsH_3 flow rate during InAs layer growth. In the low temperature region, the decrease in the FWHM of the PL peak with increase in temperature implies the suppression of non-predominant QD emissions due to carrier tunneling between nearby dots. Further increasing the temperature increases the FWHM due to the increasing effect of phonon–electron scattering. Transition energies from all relevant portions of the samples were observed in the PR spectra from 8 to 300 K. The QW transition energies obtained herein correlate with the theoretical values calculated using the $\boldsymbol{k} \cdot \boldsymbol{p}$ method. One to three transition energies in the QDs, depending on the dot size, were observed in the PR spectra.

Acknowledgement

This work was supported by the National Science Council of the Republic of China under contract No. NSC 90-2112-M006-029.

1) M. C. Chen, H. H. Lin and C. W. Shie: J. Appl. Phys. **83** (1998) 3061.
2) Y. T. Dai, J. C. Fan and Y. F. Chen: J. Appl. Phys. **82** (1997) 4489.
3) H. Lee, W. Yang and P. C. Sercel: Phys. Rev. B **55** (1997) 9757.
4) E. R. Glaser, B. R. Bennett, B. V. Shanabrook and R. Magno: Appl. Phys. Lett. **68** (1996) 3614.
5) P. Chen, Q. Xie, A. Madhukar, Lichen and A. Konkar: J. Vac. Sci. Technol. B **12** (1994) 2568.
6) D. I. Lubyshev, P. P. Gonzalez-Borrero, E. Marega, Jr., E. Petitprez and P. Basmaji: J. Vac. Sci. Technol. B **14** (1996) 2212.
7) D. I. Lubyshev, P. P. Gonzalez-Borrero, E. Marega, Jr., E. Petitprez, N. La Scala and P. Basmaji: Appl. Phys. Lett. **68** (1996) 205.
8) T. Anan, K. Nishi and S. Sugou: Appl. Phys. Lett. **60** (1992) 3159.
9) *See Materials Aspects of GaAs and InP Based Structures*, eds. V. Swaminathan and A. T. Macrander (Prentice Hall, New Jersey, 1991) p. 18.
10) Landolt-Bornstein: *Numerical Data and Functional Relationships in Science and Technology* (New series), ed. O. Madelung (Springer-Verlag, Berlin, 1987) Vol. III/22*a*, p. 117.